

# Molecular dynamics simulation of synchronization of a driven particle

Tiare Guerrero\* and Danielle McDermott<sup>†</sup>

*Department of Physics, Pacific University, Forest Grove, Oregon 97116*

(Dated: April 12, 2021)

## Abstract

We discuss a molecular dynamics simulation of a single particle moving through a viscous liquid while being driven across a washboard potential energy landscape. Our results show many dynamical patterns as the landscape and driving force are altered. For certain conditions, the particle velocity and location are synchronized or phase-locked, forming closed orbits in phase space. Quasi-periodic motion is common, for which the dynamical center of motion shifts the phase space orbit. Isolating synchronized motion in simulations and table-top experiments, can be used to study complex natural behaviors which play an important role in many physical processes.

## I. INTRODUCTION

Synchronization is a universal phenomena in which individual oscillators change frequency due to external stimuli.<sup>1</sup> The flickering patterns of candle flames mediated by temperature fluctuations,<sup>2</sup> the vibrations of singing wine glasses interacting through sound waves,<sup>3</sup> and metronomes vibrating through a supporting platform<sup>4</sup> are examples of in-phase coupled oscillations. Biological systems benefit from cooperative synchronization – birds coordinate wing flaps to optimize energy use during flight,<sup>5</sup> frogs alternate croaking patterns,<sup>6</sup> humans clap in time with music,<sup>7</sup> and at a cellular level, neurons simultaneously fire in cardiac muscle<sup>8</sup> and brain tissue.<sup>9</sup> External forcing can cause or regulate synchronization. For example, an electrical pacemaker regulates a heart beat and a pulsed light modifies the flashing pattern of fireflies.

The model discussed in this paper resembles an externally forced pendulum. A single pendulum may swing in time with an driving force like a pushed child on a swing, and may be damped by mechanical friction. Synchronized phase-locking or mode-locking first appeared in the scientific literature in 1665 with Huygens’ experiments on the motions of synchronized pendula in wall-mounted clocks.<sup>10</sup> Clock pendula swing in phase when coupled through shared vibrations. A locked-mode is an integer frequency ratio. In Huygens clocks, the pendula were observed to swing at the same rate in the same direction (1:1 mode) or opposite directions ( $-1:1$  mode). A 2:1 mode occurs when a simple pendulum four times the length of another swings with twice the period. Many subsequent simulations and laboratory experiments have revealed mode-locked synchronization in a diverse range of oscillation phenomena.

Colloid particles in complex environments are an excellent model system to explore the dynamics of mode-locking. In experiments typical colloids are plastic spheres suspended in de-ionized water or silica beads suspended in organic solvent. Colloids can be trapped with radiation pressure from a laser beam.<sup>14</sup> A colloid in such a confining region, an optical trap, oscillates about a equilibrium point. A colloid centered in an optical trap is uniformly bombarded by photons. Off-center colloids experience a net force due to uneven photon collisions across the particle surface. Depending on the location of the particle in the trap, the radiation pressure either moves colloids toward the center or ejects it from the trap. Diffraction gratings can create more complex light environments, such as periodic patterns of

minima suitable for synchronization studies.<sup>15</sup> A driven colloid can demonstrate synchronized motion within one trap, or synchronized hopping between multiple traps.

Colloids have been shown to provide an ideal system to control and study phase-locked motions at a single particle level.<sup>12,13</sup> While many systems oscillate, trapped colloids are useful for providing controlled measurements of the step-by-step dynamics of particle motion. Since colloids are large and move slowly, particle positions can be measured in real time with an optical camera.<sup>11</sup> Simulations provide complementary information, where environmental and driving parameters may be precisely and quickly modified to explore the many oscillation patterns. In the following study, we confine colloids to move along a periodic light pattern with minima and maxima defined by a sine wave, a washboard potential energy substrate.

A colloid driven across a periodic substrate may synchronize its location to the pattern of the external drive. When a constant or dc drive is applied, the particle velocity is modulated by the potential energy landscape exerted on the particle. Below some threshold the dc force is not strong enough to push the particle across a potential maximum so the average velocity is zero, a phenomena referred to as pinning.<sup>16</sup> Above the pinning threshold, a dc driven particle increases its speed at a rate proportional to the external drive. When the applied force varies periodically, an ac drive, the particle can hop back and forth across the landscape minima. Many synchronized patterns occur, controlled by the substrate pattern and driving force. When a particle is driven by combined ac and dc forces, mode-locking appears where the average particle velocity is fixed for a range of dc drive forces.<sup>17</sup>

In this paper we discuss numerical simulations of the mode-locked dynamics of a confined particle driven over a washboard shaped potential energy landscape. The numerical model is presented in Sec. II and our results are summarized in Sec. III. In Sec. IV we relate our results to a broad variety of physical systems beyond optically trapped colloids. We include problems for interested readers in Sec. V.

## II. SIMULATION

We use a classical model for studying the dynamics, using the net force on a particle to calculate its trajectory. The particle is confined in a two-dimensional simulation of area  $A = L \times L$ , where  $L = 46.6 a_0$  and  $a_0$  is a dimensionless unit of length. (In the simulations we set  $a_0 = 1$ .) The particle has position  $\vec{r} = x\hat{x} + y\hat{y}$  and velocity  $\vec{v} = d\vec{r}/dt$ . The edges

of the system are treated by periodic boundary conditions, such that a particle leaving the edge of the system is mapped back to a position within the simulation boundaries by the transformation  $x + L \rightarrow x$  and  $y + L \rightarrow y$ . We show a schematic of the system in Fig. 1(a). The units of the simulated variables are summarized in Table I.

We confine the particles using a position dependent potential energy, called a landscape or substrate. The landscape is modulated in the  $y$ -direction by the periodic function

$$U(y) = U_0 \cos(2\pi y/\lambda), \quad (1)$$

where  $\lambda = L/N_p$ , with  $N_p$  equal to the number of periods, and  $U_0$  is a parameter that sets the depth of the minima with simulation units of energy  $E_0$ . We plot this function in Fig. 1 for  $N_p = 3$ . In Fig. 1(a) we show the  $x$ - $y$  plane with a contour plot of  $U(y)$  to illustrate the 2D potential energy landscape; the maxima are colored gray and the minima colored white.

The confining force on the particle  $i$  is given by

$$\vec{F}_\ell(\vec{r}) = -\vec{\nabla}U(\vec{r}), \quad (2)$$

where  $\ell$  denotes the landscape. In Fig. 1(b) we plot  $U(y)$  to illustrate how the magnitude  $|\vec{F}_\ell|$  is calculated from the particle position  $y$ .

The particle is subject to an external time-dependent driving force  $\vec{F}_d(t)$  applied parallel to the  $y$ -direction. We model this force as

$$\vec{F}_d(t) = [F_{dc} + F_{ac} \sin(\omega t)] \hat{y}, \quad (3)$$

with a constant component  $F_{dc}$  and a time dependent component with amplitude  $F_{ac}$  and angular frequency  $\omega = 2\pi f$ .

The inertia of the small particle is reduced by interactions with the fluid particles.<sup>18</sup> We assume colloids are overdamped so the particle does not accelerate, that is, it is suspended in a continuous viscous fluid that dissipates energy supplied externally. Newton's second law for the particle is simplified by the assumption that  $\vec{a}$  is zero. The overdamped equation of motion for the velocity  $\vec{v}$  of an isolated particle is

$$\eta \vec{v} = \vec{F}_\ell(\vec{r}) + \vec{F}_d(t), \quad (4)$$

with friction coefficient  $\eta = 1$  in units of  $v_0/F_0$ . The term  $-\eta \vec{v}$  is a drag force that models energy dissipation due to the fluid. We discuss models for a sphere moving through a fluid in Problem 3.

The equation of motion provides a direct calculation of the velocity of an individual particle at position  $\vec{r}$  and simulation time  $t$ . At each time step we evaluate the net force on the particle as a function of its position  $\vec{r}(t)$  and then integrate the equation of motion to move the particle to its updated position. Because the acceleration is zero, the integration of the equation of motion is performed using the simple first-order Euler method

$$\vec{r}(t + \Delta t) = \vec{r}(t) + \vec{v}(t)\Delta t \quad (5)$$

for a time step  $\Delta t = 0.1 \tau$ . In Problem 1 we describe the numerical methods for solving differential equations such as Eq. (5).

### III. MODE-LOCKING OF A SINGLE PARTICLE

Here we drive a single particle across the landscape. The numerical implementation of the force due to the landscape is calculated using Eqs. (1) and (2)

$$F_{\ell y}(y) = A_p \sin(2\pi y/\lambda), \quad (6)$$

where the force is scaled by the parameter  $A_p = 2\pi U_0/\lambda$ . In this section we fix the landscape parameters to  $A_p = 0.1 F_0$  with  $N_p = 20$  minima, corresponding to a spatial period  $\lambda = 2.3 a_0$ . The competition between the driving force and the landscape potential can produce a variety of hopping patterns in the particle motion. The relative values of  $F_{ac}$ ,  $F_{dc}$ , and  $A_p$  control the rate and distance a particle moves forward and backward in the landscape. If  $F_d(t) > A_p$ , a particle can overcome the barrier height of the landscape, and the particle hops between minima in the energy landscape. If the driving frequency is low, as in Fig. 2, the driven particle moves in a pattern with the same frequency as the time-dependent force  $F_d(t)$ , but is modulated by the landscape period. We explore changes in the frequency and different values of  $F_{ac}$  in Problem 2. Here we vary  $F_{dc}$  while holding the remaining parameters fixed.

In Fig. 2(a) we plot  $F_d(t)$  as a function of time with the constants  $F_{dc} = 0.07$ ,  $F_{ac} = 0.07$  and  $f = 0.01$  cycles per time unit  $\tau$ . The temporal period of the driving force is  $T = 1/f = 100 \tau$ . In Fig. 2(b) we show the  $y$ -position of the particle as a function of time, where we have normalized  $y$  by  $\lambda$ . The initial particle position is  $y = 0$ . The particle moves in the positive  $y$ -direction through a distance  $\Delta y = \lambda$  in the time  $T$ , so that the average velocity

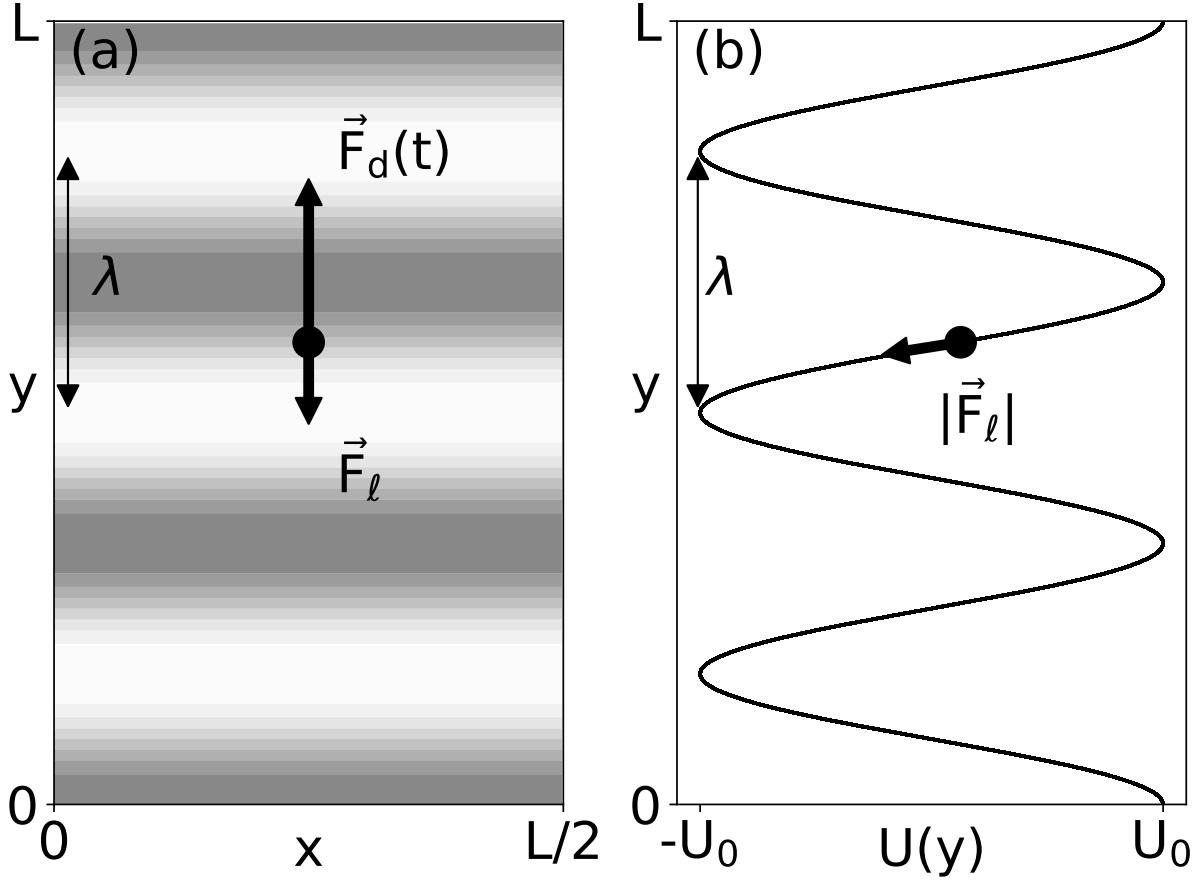


FIG. 1. Schematic of the simulation of a single particle driven across a washboard potential energy landscape. (a) View of the  $x$ - $y$  plane. The time-dependent applied driving force  $\vec{F}_d$  is parallel to the  $y$ -axis. The landscape is shown with maxima of the potential energy in gray and minima in white. The particle is subject to competing forces of the landscape and the applied driving force. (b) The potential energy function  $U(y)$ . The particle in (a) is shown at the same  $y$ -position in (b). The slope of  $U(y)$  is the magnitude of the force  $\vec{F}_\ell$ .

$\langle v_y \rangle = \lambda f$ . The inset of Fig. 2(b) shows  $y$  over one period  $100\tau < t < 200\tau$  with the contour plot described in Fig. 1(a). The motion is synchronized such that the driving force is a maximum when the landscape force is minimum, as shown by the coincidence of the steep slope of  $y/\lambda$  and the maxima in  $F_d(t)$ . When  $F_d(t)$  is large, the particle moves across the substrate maxima.

To explore the possible hopping patterns, we sweep through a range of  $F_{dc}$  for fixed  $F_{ac}$  and  $A_p$ . In Fig. 3 we increase  $F_{dc}$  in increments of  $0.001 F_0$ , and measure the average

TABLE I. Simulation parameters and units with comparable experimental values.<sup>12,13</sup> The substrate is scaled by our force units, while an experimental landscape is scaled by the Brownian motion of the particles.

Quantity	Simulation Units	Experimental values
length	$a_0 = 1$	$a_0 \sim 1.5\mu\text{m}$
energy	$E_0 = 1$	
force	$F_0 = E_0/a_0$	
time	$\tau = \eta a_0/F_0$	$\tau \sim 3\text{ s}$
velocity	$v_0 = a_0/\tau$	$v \sim 5\mu\text{m/s}$
substrate period	$\lambda = 2.3 a_0$	$\lambda = 3.5\mu\text{m}$
substrate amplitude	$A_p = 0.1 F_0$	$U_0 = 25k_B T \sim 1\text{ J}$
temperature	$T = 0$	$T \sim 290\text{ K}$

velocity  $\langle v_y \rangle$  as a function of  $F_{\text{dc}}$ . We also perform the sweep for a non-oscillatory drive  $F_{\text{ac}} = 0$ . With no oscillating component of the driving force, the force-velocity relation increases monotonically above the depinning threshold  $F_c$  such that

$$\langle v_y \rangle \propto (F_{\text{dc}} - F_c)^{-\beta}, \quad (7)$$

where the power  $\beta$  varies with the type of phase transition and may be used to identify the universality class.<sup>16</sup> The critical force  $F_c$  is equal to the maximum substrate force  $A_p$ .

The addition of an ac drive leads to the formation of modes. A mode is a periodic pattern of hops with a constant average particle velocity,  $\langle v_y \rangle$  over a range of driving forces  $F_{\text{dc}}$ . In Fig. 3 we sweep  $F_{\text{dc}}$  with  $F_{\text{ac}} = 0.07$  and  $f = 0.01$ . Each step represents a different pattern of hops between substrate minima performed by the particle due to the landscape confinement. At low values of  $F_{\text{dc}}$ , the average velocity  $\langle v_y \rangle$  is zero. Because  $A_p$  is large compared to the extrema of  $F_d(t)$ , the particle oscillates back and forth in a single minima with no net velocity, an example of a 0:0 mode. At higher values of  $F_{\text{dc}}$ , the particle velocity  $\langle v_y \rangle$  increases in steps of uniform height,  $\langle v_y \rangle = n\lambda f$ , where  $n$  is an integer. We observe a mode of  $n = 1$  for  $0.05 < F_{\text{dc}} < 0.08$ ,  $n = 2$  for  $0.08 < F_{\text{dc}} < 0.11$ ,  $n = 3$  for  $0.12 < F_{\text{dc}} < 0.13$ ,  $n = 4$  for  $0.14 < F_{\text{dc}} < 0.155$ , and  $n = 5$  for  $0.155 < F_{\text{dc}} < 0.16$ . Higher modes are not visible. The step width is nonlinear and depends on the strength of  $F_{\text{ac}}$  for this landscape potential.<sup>13,30</sup>

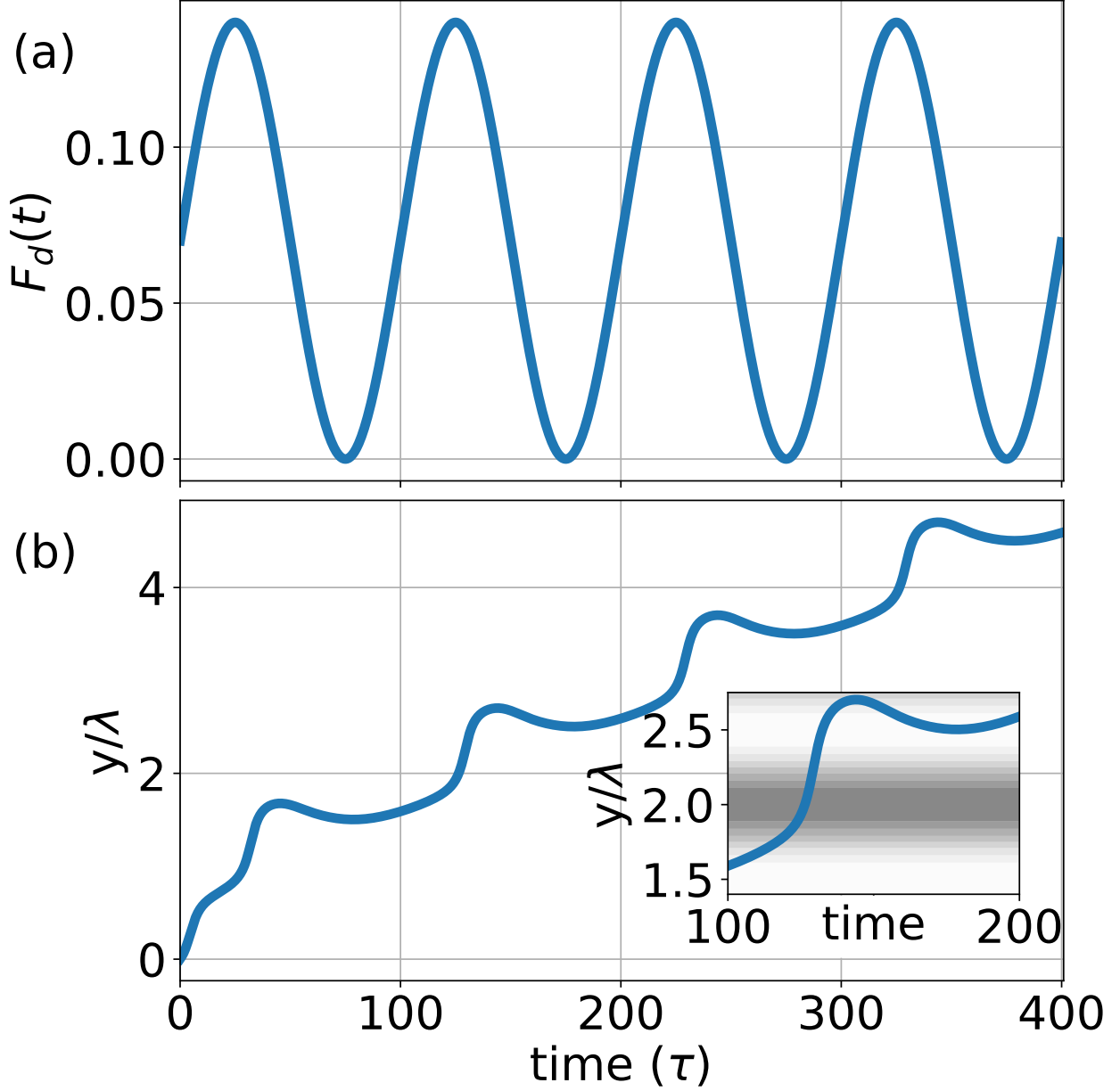


FIG. 2. (a) The applied driving force  $F_d(t)$  with parameters  $F_{dc} = 0.07$ ,  $F_{ac} = 0.07$  and  $f = 0.01$ . (b) The  $y$ -position of the driven particle normalized by the period of the substrate  $\lambda$ . The substrate strength is  $A_p = 0.1$ . The inset shows the  $y$ -position through the second period  $100\tau < t < 200\tau$  along with the contour plot depicting the landscape potential described in Fig. 1(a).

These steps, known as Shapiro steps, can have a variety of interesting patterns such as a devil's staircase related to chaotic dynamics.<sup>19</sup>

To study synchronization patterns, it is useful to compare mode-locked quantities in a two-dimensional phase plot. For a driven pendulum confined to a single potential well, an



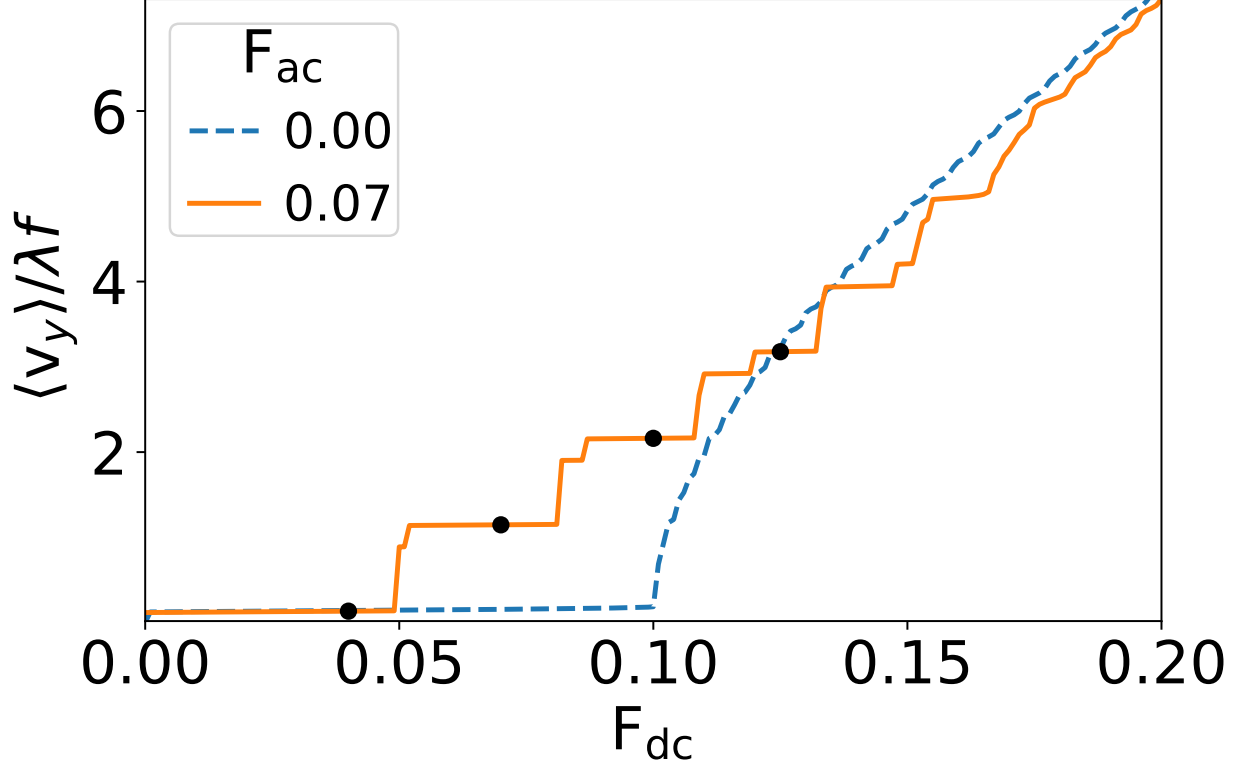


FIG. 3. Average particle velocity  $\langle v_y \rangle$  as a function of  $F_{dc}$ . We let  $F_{ac} = 0.0$  (blue dashed) and  $F_{ac} = 0.07$  (orange) with  $f = 0.01$  as in Fig. 2. The value of  $F_{dc}$  for the first four steps correspond to the fixed value of  $F_{dc}$  in each of the phase plots in Fig. 4(a-d).

appropriate phase space is the particle velocity  $v_y$  versus the position  $y$ . For a particle driven through multiple identical wells we define phase variables to account for the net increase in the position. The phase position is

$$\phi(t) = 2\pi[y(t) - \langle v_y \rangle t]/\lambda, \quad (8)$$

centered about the average particle displacement  $\langle v_y \rangle t$  and normalized by the substrate period  $\lambda$ .<sup>12</sup> The phase velocity is

$$\dot{\phi}(t) = 2\pi[v_y(t) - \langle v_y \rangle]/\lambda. \quad (9)$$

For a zero landscape force, the phase velocity is zero when  $F_d(t) = F_{dc}$ . If the system is strictly mode-locked, the particle velocity recurs at a particular spatial location, and a closed loop appears in phase space. A 1:1 mode appears as a circle or oval. Nodes appear for higher modes, sometimes forming figure-eights or other recognizable patterns. A system

that is nearly phase locked will appear as an almost closed loop. Such quasiperiodic systems are not fully synchronized so the position-velocity relation shifts in time as in Fig. 4.

In Fig. 4 we plot  $\dot{\phi}(t)$  versus  $\phi(t)$  for increasing  $F_{dc}$ , with the remaining parameters fixed as in Fig. 2. For  $F_{dc} = 0.04$  the phase plot in Fig. 4(a) is an asymmetric curve. A tail appears due to the initial transient motion of the particle. The particle is confined to a single substrate minima, and has no net velocity. The asymmetry is caused by the bias induced by  $F_{dc}$ . In Fig. 4(b) with  $F_{dc} = 0.07$  the phase loop is a symmetric triangular shape, indicating a 1:1 match between the particle motion and velocity consistent with Fig. 2(a). As  $F_{dc}$  is increased, nodes form in the phase diagram, which occur due to repeated values of  $\dot{\phi}$  over multiple phase positions. In Fig. 4(c) with  $F_{dc} = 0.1$  two nodes form. The particle moves a distance  $2\lambda$  during one time period. For  $F_{dc} = 0.125$  as in Fig. 4(d), three nodes form as the particle moves across  $3\lambda$ .

#### IV. CONCLUSION

A single particle driven across a periodic potential landscape synchronizes its motion to environmental and external forces. Our simulations reproduce the experiments and simulations presented in Juniper *et al.*<sup>12,13</sup> of mode locking in driven colloids on a periodic optical landscape. The model is easy to simulate yet relevant to a broad range of condensed matter systems. Colloids are relatively easy to manipulate and image in experiments, making ideal proxies for systems such as cold atoms or electron gases.<sup>15</sup> Dynamical mode-locking is observed in technologies such as quantum electronic devices as stepped regions in the relation between current and voltage, where the voltage is the analog of the external driving force and current is the analog of particle velocity. Known as Shapiro steps, these mode-locked or phase-locked currents were first observed in single Josephson junctions<sup>27,28</sup>. Shapiro steps vary in width depending on the strength of the applied ac forces, and are observed in a variety of ac and dc driven systems displaying non-Ohmic behavior in voltage-current curves, including charge density waves, spin density waves and superconducting vortices in landscapes engineered with periodic patterns of pinning sites.<sup>30</sup>

Mode-locking is a useful probe of complex quantum mechanical systems because the motions of individual particles can be inferred only from other measurements. Our results are relevant to synchronization effects in a broad range of experimental systems including

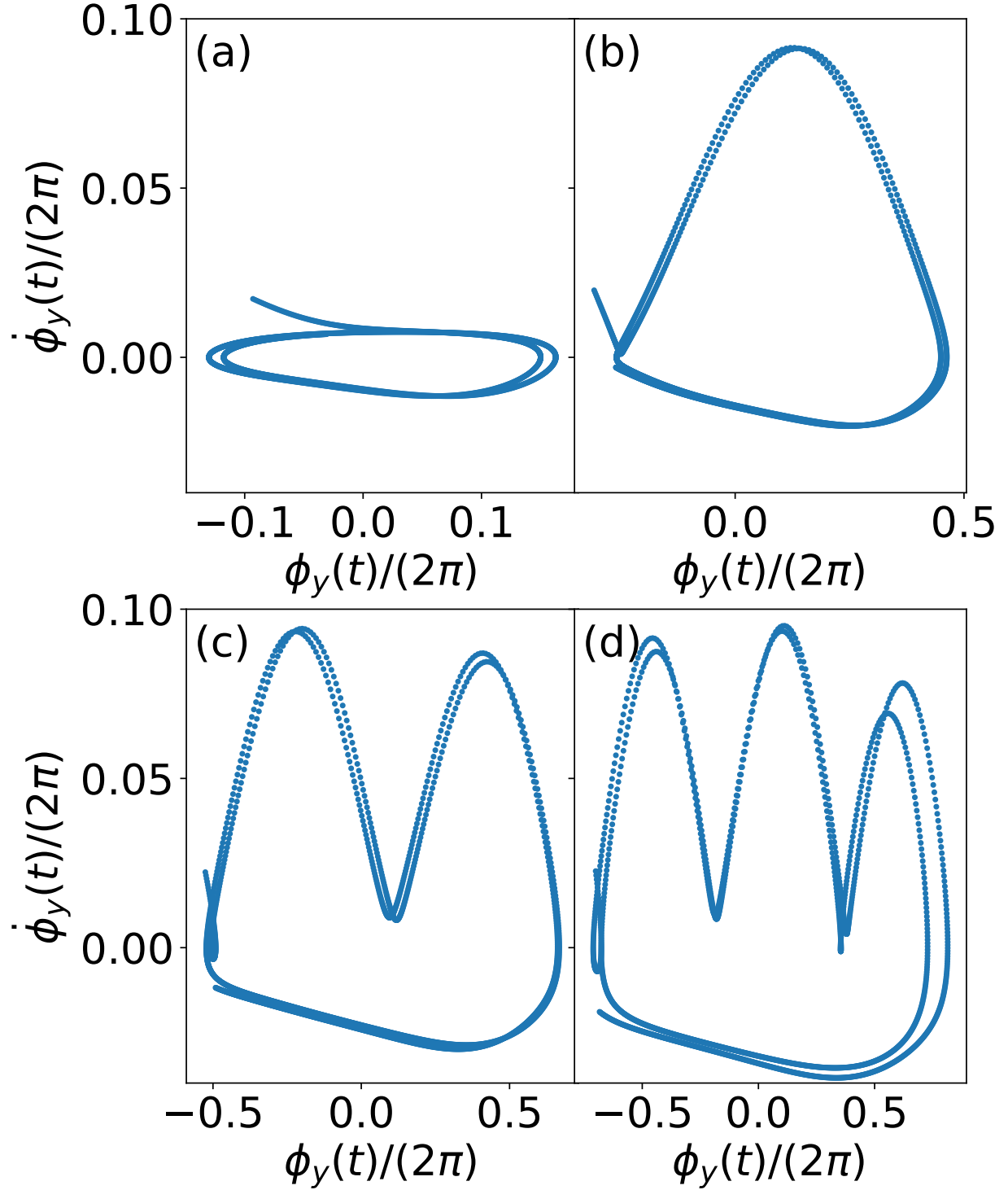


FIG. 4. Phase plot of  $\dot{\phi}(t)/(2\pi)$  versus  $\phi(t)/(2\pi)$ . The particle is driven with  $F_{\text{dc}}$  equal to (a) 0.04, (b) 0.07, (c) 0.1, and (d) 0.125. These values are denoted as black circles in Fig. 3. The other parameters are  $F_{\text{ac}} = 0.07$ ,  $f = 0.01$ , and  $A_p = 0.1$  as in Fig. 2.

optically confined colloids, superconductors with periodic pinning arrays, and the charge and spin of atomic systems.

## V. SUGGESTED PROBLEMS

In the following we explore the behavior of our model with suggested problems for interested readers. We discuss the molecular dynamics algorithm and numerical integration techniques in Problem 1. Changes to the parameters are described in Problem 2. We include analytic solutions to the linear drag equation in Problem 3, and consider the equation of motion in Problem 4. We extend the numerical model to include finite temperature effects in Problem 5.

*Problem 1.* Write your own MD code

To calculate the position of the particle as a function of time, we numerically integrate the equation of motion, Eq. (4), using the standard definition of velocity  $\vec{v} = d\vec{r}/dt$  using the Euler method. Equation (4) provides a direct calculation for the particle velocity from the net force on the particle, as demonstrated in Problem 4.

A working example of this code is available in Ref. 24. If you would like to write your own code, the following guide will walk you through our choices. In the code excerpts, most comments and optional details are removed for clarity. We use the Python language for educational purposes. To model many particles, we recommend a compiled language to perform the many operations associated with neighbor lists to compute particle interactions.

- (a) **Initialization.** For convenience, we define a Python dictionary to contain the simulation constants that could easily be passed by reference to subroutines. We have left as an exercise the addition of the remaining parameters of the system.

```
def set_parameters():
    '''set simulation parameters...'''
    #declare the dictionary
    dict={}
    dict['dt'] = 0.1 #time step in simulation units
    #control the oscillating component of driving force
    dict['F_AC'] = 0.07 #amplitude of force oscillation
```

```

dict['freq'] = 0.01 #frequency of force oscillation
#...                #left as an exercise to the reader
return dict

```

The function is called at the top of the main function followed by a call to a subroutine containing the MD algorithm.

```

if __name__ == "__main__":
    parameters = set_parameters()
    #run the MD simulation
    single_particle(parameters)

```

- (b) **Time loop.** The Euler method is effective for solving linear ordinary differential equations of the form  $dy/dt = f(t, y(t))$  with the initial condition  $y(t_0) = y_0$ . The solution is calculated by stepping in time through  $n$  integer steps  $t_n = t_0 + n\Delta t$ . At each subsequent step the new value for  $y$  is calculated as a solution of a map using discrete times  $y_{n+1} = y_n + f(t_n, y_n)$ . Apply the Euler method to Eq. (4) to determine the analytic expression for the position of a particle  $y_n$  at the  $n$ th time step.

Add a **for** loop to step through each integer time step. This loop controls the flow of the program and retains information for the particle position and other properties as a function of time. Assume this information will be calculated in a subroutine.

We used the subroutine **single\_particle()** to calculate the lengths of the arrays that contain the position, velocity, and time data. The lengths of these arrays are affected by how much data you choose to save (see comment following sample code). Define a loop to calculate the particle position and velocity through each time step, calculated in the subroutine **md\_step()** which will be described in more detail in (c).

```

def single_particle(parameters, plot="y-position"):
    '''Run MD simulation...'''
    #define empty arrays to hold data as a function of time
    #(left as an exercise to the reader)
    #loop through the integer time steps in the simulation

```

```

for int_time in range(0,maxtime):
    #(left as an exercise to the reader)
    time += dt

```

*Comment:* A key decision for any MD algorithm is how much information to save during and after the simulation. We define the following constants to manage the length of arrays containing data. We found in practice that for short simulations times we could save all data.

```

dict['maxtime']=int(40/dict['freq'])    #total time steps
dict['writemovietime']=1    #write data to arrays for plotting

```

- (c) **Position and force calculations.** We created a subroutine to consider each type of force in the system (external drive, landscape, etc). If the particle moves beyond the limits  $0 \leq y < L$ , it must be returned using the periodic boundary conditions discussed in Sec. II.

```

def md_step(y, int_time, avg_vy, parameters, ft=0):
    '''Calculate net force and integrate eq. of motion...'''
    #calculate the floating point value for time
    time = int_time * dt
    #reset vy for every time step because ay = 0
    vy = 0
    #calculate the net force on the particle
    vy = #(left as an exercise to the reader)
    #calculate the new position
    y += #(left as an exercise to the reader)
    #check periodic boundary conditions
    #(left as an exercise to the reader)
    return y, vy, avg_vy

```

The Euler algorithm can be applied to calculate reasonable numerical solutions to non-linear equations if the time step  $\Delta t$  is kept sufficiently small.<sup>23</sup> In our simulations we use the time step  $\Delta t = 0.1$  and find no change in the solution when we decrease the time step to

smaller values. In simulations of many interacting particles, a smaller time step is essential for accurate results. Particle-particle interactions are typically nonlinear, so that the inter-particle force changes significantly over small distances and the simple Euler algorithm is insufficient.

*Problem 2. Exploring model parameters*

A range of behaviors can be explored by varying the relative strength of the confining landscape and the external driving force.

- (a) Explore the effect of increasing  $F_{\text{ac}}$  on the hopping pattern. For a single driven particle, the hopping patterns are typically characterized by  $n_f$ , the number of forward steps, versus  $n_b$ , the number of backward steps in one time period. The total displacement of  $(n_f - n_b)\lambda$  is the net hop length. In Fig. 2, the particle moves forward through a minima ( $n_f = 1$ ), and does not move backward through a full minima ( $n_b = 0$ ). To achieve backward hops, the ratio of  $F_{\text{ac}}/F_{\text{dc}}$  must be greater than one and the difference  $|F_{\text{ac}} - F_{\text{dc}}| > A_p$ . Hold all other parameters fixed and explore how the hopping pattern changes for increasing  $F_{\text{ac}}$ . For example, calculate the patterns of hops for  $f = 0.01$ ,  $F_{\text{dc}} = 0.07$ , and  $A_p = 0.1$  and  $F_{\text{ac}} = 0.2, 0.3$  and  $0.4$ .
- (b) Explore the effect of increasing the driving frequency on the hopping pattern. In Sec. III the frequency is sufficiently low so that the effect of the applied force is large over a sustained time interval, allowing the particle to hop a substrate maxima. For example fix the parameters  $F_{\text{dc}} = 0.1$ ,  $F_{\text{ac}} = 0.05$ , and  $A_p = 0.1$  and explore high frequency ( $f = 0.1$ ), intermediate frequency ( $f = 0.01$ ), and low frequency ( $f = 0.005$ ).
- (c) Explore the effect of increasing  $F_{\text{ac}}$  on the step pattern in Fig. 3. For example, sweep the driving force  $F_{\text{dc}}$  over increments of  $\Delta F_{\text{dc}} = 0.001$  for  $F_{\text{ac}}$  and frequency  $f = 0.01$ . Appropriate values for  $F_{\text{ac}}$  in the range  $[0.1, 0.4]$  will demonstrate a change in the step width in a plot of  $\langle v_y \rangle$  versus  $F_{\text{dc}}$ .

*Problem 3. Drag models and Reynolds numbers*

Stokes' law describes the drag force  $\vec{F}_{\text{lin}} = -3\pi\eta D\vec{v}$  on a sphere moving through a viscous liquid at velocity  $\vec{v}$ , where  $\eta$  is the dynamic fluid viscosity and  $D$  is the particle diameter.<sup>20</sup> In simulations we subsume the constants  $3\pi D$  such that  $3\pi D\eta \rightarrow \eta$ . Often drag forces are

modeled as a polynomial series<sup>20</sup>  $\vec{F}_{\text{drag}} = -b\vec{v} - cv^2\hat{v} + \dots$ . Truncating the series at the first term is justified by demonstrating the sphere has a low Reynolds number  $R = Dv\rho/\eta$ , where  $\rho$  is the fluid density and  $v$  is the particle's speed. If  $R$  is small, the quadratic and higher order terms may be ignored.

Use reasonable values for the experimental analog of this system and show that the Reynolds number is small. In addition to the values listed in Table I, the viscosity is  $\eta \sim 10^{-3}$  Pa-s,<sup>21</sup> and the liquid density  $\rho \sim 10^3$  kg/cm<sup>3</sup>.<sup>22</sup>

*Problem 4. Equation of motion*

Newton's second law states that the acceleration of a particle is proportional to the sum of the forces on the particle,  $m\vec{a} = \sum \vec{F}$ , where  $m$  is the inertial mass. The addition of a dissipative force to a dynamical equation of colloid motion is typically modeled by a drag force proportional to the particle's velocity in the opposite direction of motion  $\vec{F}_{\text{drag}} = -\gamma\vec{v}$ , where  $\gamma = 3\pi\eta D$  is the drag coefficient described in Problem 3. The ratio of  $m/\gamma$  is the momentum relaxation time, and is small for particles with low Reynolds numbers. The mass of a typical colloid particle is 15 picograms, leading to a momentum relaxation time on the order of microseconds.

- (a) Given the values listed in Table I, show that the momentum relaxation time is  $m/\gamma \approx 0.5 \mu\text{s}$ .
- (b) If  $m/\gamma$  is small, the particle's acceleration can be ignored entirely. Using Newton's second law for a small momentum relaxation time, show that a particle confined to a landscape exerting force  $F_\ell(\vec{r})$  subject to a time dependent drive  $F_d(t)$  can be modeled by the equation of motion in Eq. (4).

*Problem 5. Brownian motion*

Brownian motion describes the apparent random motion of visible particles due to collisions with invisible fluid particles. The rate of collisions depends on the temperature, viscosity and the density of the suspending fluid.<sup>25</sup> An optically trapped colloid executing Brownian motion is a useful probe of microscopic forces.<sup>21</sup>

In simulations it is common to treat the invisible fluid particles as a continuous fluid to reduce the computational expense. Temperature effects can be modeled by applying randomized forces  $f_T$ , where  $T$  denotes temperature, to the visible particles. We use the



normal distribution to generate a series of  $f_{T_n}$  values for each time step  $n$ .<sup>26</sup> A normalized random distribution of forces causes fluctuations in the motion equally in all directions such that the force  $f_T$  averaged over a finite time interval is zero. In one dimension we have  $\langle f_T(t) \rangle = \frac{1}{N} \sum_n^N f_{T_n} = 0$ , where the integer  $n$  indicates the number of time steps and  $t = N\Delta t$ . A particle with sufficient energy  $k_B T_{\min}$  may hop over landscape barriers. In our simulations, we let  $k_B T/E_0 \rightarrow T$ , with the constants set to unity to compare directly with the force.

For zero applied driving force, find the minimum temperature required for a single particle to hop over the maxima in the potential landscape. Assume that the particle is confined to move along the  $y$ -direction and include Brownian motion. Appropriate temperatures to explore are  $3.0 < T/A_p = 7.0$ . Plot the  $y$  position versus time for this particle.

For a driven particle, we ignore the effects of temperature in these simulations. We note that even for  $T/A_p = 6.0$ , the hopping rate is much less than the frequency of the applied drive. At sufficiently high temperatures, Brownian motion does affect the formation of mode-locked steps and can be observed in experiments.

## ACKNOWLEDGMENTS

Charles and Cynthia Reichhardt inspired the project and provided the original molecular dynamics code written in C. We acknowledge funding from the M.J. Murdock Charitable Trust and the Pacific Research Institute for Science and Mathematics.

---

\* guer9330@pacificu.edu

† mcdermott@pacific.edu

<sup>1</sup> A. Pikovsky, M. Rosenblum, and J. Kurths, *Synchronization: A Universal Concept in Nonlinear Sciences* (Cambridge University Press, Cambridge, 2003).

<sup>2</sup> K. Okamoto, A. Kijima, Y. Umeno, and H. Shima, “Synchronization in flickering of three-coupled candle flames,” *Sci. Rep.* **6**, 36145–36155 (2016).

<sup>3</sup> T. Arane, A. K. R. Musalem, and M. Fridman, “Coupling between two singing wineglasses,” *Am. J. Phys.* **77**, 1066–1067 (2009).

- <sup>4</sup> J. Jia, Z. Song, W. Liu, J. Kurths, and J. Xiao, “Experimental study of the triplet synchronization of coupled nonidentical mechanical metronomes,” *Sci. Rep.* **5**, 17008–17020 (2015).
- <sup>5</sup> S. Portugal, T. Hubel, J. Fritz, S. Heese, D. Trobe, B. Voelkl, S. Hailes, A. M. Wilson, and J. R. Usherwood, “Upwash exploitation and downwash avoidance by flap phasing in ibis formation flight,” *Nature* **505**, 399–402 (2014).
- <sup>6</sup> I. Aihara, T. Mizumoto, T. Otsuka, H. Awano, K. Nagira, H. G. Okuno and K. Aihara, “Spatio-temporal dynamics in collective frog choruses examined by mathematical modeling and field observations,” *Sci. Rep.* **4**, 3891–3899 (2014).
- <sup>7</sup> P. Tranchant, D. T. Vuvan, and I. Peretz, “Keeping the beat: A Large sample study of bouncing and clapping to music,” *PLoS ONE* 11(7): e0160178 (2016).
- <sup>8</sup> G. Martin Hall, Sonya Bahar, and Daniel J. Gauthier, “Prevalence of rate-dependent behaviors in cardiac muscle,” *Phys. Rev. Lett.* **82**, 2995–2998 (1999).
- <sup>9</sup> W. Singer, “Striving for coherence,” *Nature* **397** 391–393 (1999).
- <sup>10</sup> M. Bennett, M. F. Schatz, H. Rockwood, and K. Wiesenfeld, “Huygens’ clocks,” *Proc. Roy. Soc. A* **458**, 563–579 (2002).
- <sup>11</sup> A. Pertsinidis and X. Ling, “Equilibrium configurations and energetics of point defects in two-dimensional colloidal crystals,” *Phys Rev. Lett.* **87**, 098303-1–4 (2001).
- <sup>12</sup> M. P. N. Juniper, A. V. Straube, R. Besseling, D. G. A. L. Aarts, and R. P. A. Dullens, “Microscopic dynamics of synchronization in driven colloids,” *Nat. Commun.* **6**, 7187–7194 (2015).
- <sup>13</sup> M. P. N. Juniper, U. Zimmermann, A. V. Straube, R. Besseling, D. G. A. L. Aarts, H. Löwen, and R. P. A. Dullens, “Dynamic mode locking in a driven colloidal system: Experiments and theory,” *New J. Phys.* **19** (1), 013010-1–14 (2017).
- <sup>14</sup> A. Ashkin, “Optical trapping and manipulation of neutral particles using lasers,” *Proc. Natl. Acad. Sci. U.S.A.* **94**, 4853–4860 (1997).
- <sup>15</sup> D. G. Grier, “A revolution in optical manipulation,” *Nature* **424**, 810 (2003).
- <sup>16</sup> C. Reichhardt and C. J. Olson Reichhardt, “Depinning and nonequilibrium dynamic phases of particle assemblies driven over random and ordered substrates: a review,” *Rep. Prog. Phys.* **80**, 026501-1–64 (2017).
- <sup>17</sup> C. Reichhardt, and C. J. O. Reichhardt, “Shapiro steps for skyrmion motion on a washboard potential with longitudinal and transverse ac drives,” *Phys. Rev. B* **92** (22), 224432-1–12 (2015).

- <sup>18</sup> E. M. Purcell, “Life at low Reynolds numbers,” *Am. J. Phys.* **45**, 3–11 (1977).
- <sup>19</sup> P. Bak. “The Devil’s staircase,” *Physics Today* **39**(12), 38–45 (1986).
- <sup>20</sup> J. Taylor, *Classical Mechanics* (University Science Books, 2005).
- <sup>21</sup> G. Volpe and G. Volpe, “Simulation of a Brownian particle in an optical trap,” *Am. J. Phys.* **81**(3), 224–230 (2013).
- <sup>22</sup> IAPWS R12-08, “Release on the IAPWS formulation 2008 for the viscosity of ordinary water substance, September 2008, <<http://www.iapws.org/relguide/viscosity.html>>.
- <sup>23</sup> M. Newman, *Computational Physics* (CreateSpace Independent Publishing Platform, 2012).
- <sup>24</sup> <[https://github.com/mcddanielle/AJP\\_project/](https://github.com/mcddanielle/AJP_project/)>.
- <sup>25</sup> A. Einstein, *Investigations on the Theory of the Brownian Movement* (Dover Publications, 1956).
- <sup>26</sup> C. R. Harris, K. J. Millman, S. J. van der Walt et al., “Array programming with NumPy,” *Nature* **585**, 357–362 (2020).
- <sup>27</sup> S. Shapiro, “Josephson currents in superconducting tunneling: The effect of microwaves and other observations,” *Phys. Rev. Lett.* **11**, 80–82 (1963).
- <sup>28</sup> A. A. Golubov, M. Yu. Kupriyanov, and E. Il’ichev, “The current-phase relation in Josephson junctions,” *Rev. Mod. Phys.* **76**, 411–469 (2004).
- <sup>29</sup> S. P. Benz, M. S. Rzchowski, M. Tinkham, and C. J. Lobb, “Fractional giant Shapiro steps and spatially correlated phase motion in 2D Josephson arrays,” *Phys. Rev. Lett.* **64**, 693–696 (1990); D. Domínguez and J. V. José, “Giant Shapiro steps with screening currents,” *Phys. Rev. Lett.* **69**, 514–517 (1992).
- <sup>30</sup> C. Reichhardt, R. T. Scalettar, G. T. Zimányi, and N. Grønbech-Jensen, “Phase-locking of vortex lattices interacting with periodic pinning,” *Phys. Rev. B* **61**, R11914 (2000).